

MAGNETOSPHERIC GAMMA-RAY EMISSION IN ACTIVE GALACTIC NUCLEI

GRIGORIOS KATSOUKAKOS^{1,2,3}

FRANK M. RIEGER^{2,3}

¹*International Max Planck Research School for Astronomy and Cosmic Physics, University of Heidelberg (IMPRS-HD)*

²*ZAH, Institut für Theoretische Astrophysik, Universität Heidelberg, Philosophenweg 12, 69120 Heidelberg, Germany*

³*Max-Planck-Institut für Kernphysik, P.O. Box 103980, 69029 Heidelberg, Germany*

(Accepted December 4, 2017)

ABSTRACT

The rapidly variable, very high-energy (VHE) gamma-ray emission from Active Galactic Nuclei (AGN) has been frequently associated with non-thermal processes occurring in the magnetospheres of their supermassive black holes. The present work aims to explore the adequacy of different gap-type (unscreened electric field) models to account for the observed characteristics. Based on a phenomenological description of the gap potential, we estimate the maximum extractable gap power L_{gap} for different magnetospheric set-ups, and study its dependence on the accretion state of the source. L_{gap} is found to be in general proportional to the Blandford-Znajek jet power L_{BZ} and a sensitive function of gap size h , i.e. $L_{gap} \sim L_{BZ}(h/r_g)^\beta$, where the power index $\beta \geq 1$ is dependent on the respective gap-setup. The transparency of the black hole vicinity to VHE photons generally requires a radiatively inefficient accretion environment and thereby imposes constraints on possible accretion rates, and correspondingly on L_{BZ} . Similarly, rapid variability, if observed, may allow to constrain the gap size $h \sim c\Delta t$. Combining these constraints, we provide a general classification to assess the likelihood that the VHE gamma-ray emission observed from an AGN can be attributed to a magnetospheric origin. When applied to prominent candidate sources these considerations suggest that the variable (day-scale) VHE activity seen in the radio galaxy M87 could be compatible with a magnetospheric origin, while such an origin appears less likely for the (minute-scale) VHE activity in IC310.

Keywords: black holes — acceleration of particles — galaxies: individual (M87, IC310) — gamma rays: galaxies

arXiv:1712.04203v1 [astro-ph.HE] 12 Dec 2017

1. INTRODUCTION

Non-thermal magnetospheric processes in the vicinity of supermassive black holes (BH) have been considered to provide a promising explanatory framework for the origin of ultra-high energy cosmic rays (UHECRs) and the rapidly variable very high energy (VHE; > 100 GeV) gamma-ray emission in AGN (e.g., see [Rieger 2011](#), for review and references).

Accretion processes in AGN could support magnetic field strengths up to $B \sim 10^5$ Gauss on black hole horizon-scales r_H . A black hole embedded in such a magnetic field and rotating with angular frequency $\Omega^H = a_s c / 2r_H$, where a_s is the dimensionless black hole spin parameter, will induce an electric field of magnitude $E \sim (v_{rot}/c) \times B \sim (\Omega^H r_H / c) B \sim (a_s/2) B$ corresponding to a permanent voltage drop across the horizon of magnitude $\Delta V_{gap} \sim E r_H \sim (a_s/2) r_H B$. This provides for the general possibility of particle acceleration and an efficient electromagnetic (Poynting flux) extraction of rotational energy from the black hole (e.g., [Thorne et al. 1986](#); [Beskin & Kuznetsova 2000](#)).

It has been proposed that the presence of strong electric fields close to the supermassive black holes in AGN could also facilitate the acceleration of cosmic rays to UHE energies of $\sim 10^{20}$ eV, perhaps even after their main nuclear activity has ceased and the sources became quiescent ("dormant AGN") (e.g., [Boldt & Ghosh 1999](#); [Boldt & Loewenstein 2000](#); [Aharonian et al. 2002](#); [Levinson & Boldt 2002](#); [Neronov et al. 2009](#); [Kalashev et al. 2012](#); [Moncada et al. 2017](#)). Proposals of this sort generally require that the electric field is not significantly shortened out (i.e., that a "vacuum gap" exists) and that curvature losses do not introduce a strong suppression (cf. [Pedaletti et al. 2011](#)). Similarly, direct electric acceleration of electrons could lead to curvature and inverse Compton emission in the VHE domain, and potentially trigger a pair cascade that could short out the electric field and lead to vacuum breakdown ([Levinson 2000](#)).

Magnetospheric gamma-ray emission has recently received a particular impetus in the context of the rapidly variable VHE emission detected from misaligned AGN, most prominently from the radio galaxies M87 ($d \simeq 16$ Mpc) and IC310 ($d \sim 80$ Mpc) (e.g., [Neronov & Aharonian 2007](#); [Vincent 2010](#); [Levinson & Rieger 2011](#); [Aleksić et al. 2014a](#); [Broderick & Tchekhovskoy 2015](#); [Ptitsyna & Neronov 2016](#); [Hirotani & Pu 2016](#); [Hirotani et al. 2016](#)). This goes along with the recognition that r_g/c , where $r_g = r_s/2 = GM_{BH}/c^2$ is the gravitational radius of the black hole, provides a characteristic variability timescale of the emission in the frame of the galaxy, and that specific set-ups are needed to tap sufficient power on significantly shorter time scales (e.g.,

[Barkov et al. 2010](#); [Giannios et al. 2010](#); [Aharonian et al. 2017](#)). The day-scale VHE activity in M87 (e.g., [Aharonian et al. 2006](#); [Albert et al. 2008](#); [Acciari et al. 2009](#)) and the minute-scale one in IC310 ([Aleksić et al. 2014a](#)) correspond to scales of about $4r_g/c$ and $0.2r_g/c$, respectively. The VHE variability thus provides clear evidence for a compact emission zone, and this usually tends to be associated with smaller distance scales, i.e. a location closer to the black hole. Nevertheless, this does not necessarily have to be the case. In fact, the moderate angular resolution of VHE gamma-ray instruments ($\sim 0.1^\circ$) does not allow to spatially resolve such scales, and this introduces some uncertainties. The situation can however be improved significantly by combining VHE with high-resolution radio observations capable of probing scales down to several tens of r_g . In the case of M87 rapid VHE activity seems to precede the ejection of a radio-emitting component close to the black hole, suggesting that (at least sometimes) the VHE emission originates in the vicinity of its black hole ([Acciari et al. 2009](#)).

Misaligned AGN, with jets inclined such that Doppler factors are modest ($D \lesssim$ a few), belong to the most promising source class in this regard, as possible Doppler modifications of observed timescales are reduced and the non-thermal jet radiation does not necessarily overpower the non-boosted magnetospheric emission (cf. [Rieger 2017](#)). The observation of rapid variability on the other hand, imposes important constraints on possible gap sizes and extractable powers, and offers critical information as to the plausibility of relating the emission to a magnetospheric origin in a particular source. This is obviously of relevance for assessing the potential of different candidate sources. As we will show later on (Sec. 2), however, different realisations of the gap potential are in principle conceivable. While this complicates the picture somewhat, observations can allow to favour/disfavour some of them, thereby offering additional clues on e.g. a possible disk-BH-jet connection. Pair cascade processes in the black hole magnetosphere could possibly provide the plasma source required to ensure a force-free MHD outflow in a Blandford-Znajek type set-up ([Blandford & Znajek 1977](#); [Levinson & Rieger 2011](#)). This in principle allows to link magnetospheric processes to accretion and jet formation, and makes magnetospheric studies of general relevance for jet investigations, and vice versa.

This paper is structured as follows. In Sec. 2 basic features of the black hole environment are presented, the gap potential is evaluated for different assumptions and the respective acceleration and radiative processes are analysed. This is then used to derive a constraint on the maximum possible gap power as a function of gap

height. Application to the well-known VHE emitters M87 and IC310 is discussed in Sec. 3. The conclusions are shortly summarized in Sec. 4.

2. MAGNETOSPHERIC EMISSION

Magnetospheric emission models usually rely on efficient "gap-type" particle acceleration (but see, e.g., Rieger & Aharonian 2008; Osmanov et al. 2017, for exemptions). According to Ohm's law, $\mathbf{J} = \sigma(\mathbf{E} + \mathbf{V}/c \times \mathbf{B})$, the deficiency of electric charges (i.e., low conductivity σ) within the black hole magnetosphere can directly lead to the formation of (non-degenerate) regions with an unscreened parallel electric field component, i.e. $\mathbf{E} \cdot \mathbf{B} \neq 0$. Thus, magnetospheric particles moving along the magnetic fields into such charge-empty ("gap") regions can be strongly accelerated to high energies by these parallel electric field components. Gaps can in principle occur under several conditions. Extended gaps (with sizes $h \geq r_g$), for example, are known for the vacuum black hole magnetosphere (Wald 1974). Thinner gaps (with sizes $h < r_g$) can however exist as well and might also be expected in the context of degenerate, force-free outflows (i.e., in ideal MHD). As an example, we mention the null surface (located close to r_g) formed due to the frame-dragging effect (Beskin et al. 1992; Hirotani & Okamoto 1998) and the stagnation surface (typically located at a few r_g) which divides MHD inflow from outflow regions (e.g., Globus & Levinson 2014; Broderick & Tchekhovskoy 2015). In these places, continuous charge replenishment (by particle creation or diffusion) has to occur in order to sustain the required Goldreich-Julian charge density $\rho_{GJ} = -e n_{GJ} \simeq -\Omega^F B_{\perp}/(2\pi c)$.

Throughout this paper, we do not consider a specific gap position, but adopt a more phenomenological description. We assume that primary particles can be injected into the magnetosphere by processes in the accretion environment (e.g., via annihilation of MeV photons emitted by a hot accretion flow). As has been shown elsewhere, the injected seed particle density is not sufficient for complete screening ($n_{\pm} < n_{GJ}$) below a certain accretion rate \dot{M} (Levinson & Rieger 2011). This implies that gaps can appear if the accretion flow is advection-dominated (ADAF).

2.1. The black hole vicinity

We consider a rotating black hole of spin parameter $a_s \simeq 1$ and mass $M_{BH} = M_9 \times 10^9 M_{\odot}$ onto which gas accretion occurs. The central black hole is fed by the accretion flow at a rate $\dot{M} = \dot{m} \dot{M}_{Edd}$ expressed in Eddington units, where $\dot{M}_{Edd} = L_{Edd}/\eta_c c^2 \approx 1.4 \times 10^{27} M_9$ g s^{-1} , $L_{Edd} = 1.3 \times 10^{47} M_9$ erg s^{-1} is the fiducial Ed-

dington luminosity and $\eta_c \sim 0.1$ the canonical conversion efficiency. This corresponds to a reference limit on the accretion luminosity $L_{disk} = \eta_c \dot{M} c^2 = \dot{m} L_{Edd}$ that is comparable to the one for a steady, standard (geometrically thin, optically thick) disk. As shown later on, however, a radiatively inefficient accretion flow is a prerequisite for the escape and thus observability of magnetospheric VHE gamma-rays. For an optically-thin advection-dominated accretion flow (ADAF) in which most of the viscously dissipated energy is advected with the flow, cooling is almost inefficient, resulting in a much reduced luminosity $L_{ADAF}/L_{disk} \propto \dot{m} \ll 1$. ADAFs can only exist below a critical accretion rate, usually requiring $\dot{m}_c \simeq 0.4 \alpha_v^2 \lesssim 0.015$ (with $\alpha_v \lesssim 0.2$) (Mahadevan 1997; Narayan et al. 1998), though more restrictive conditions ($\dot{m}_c \sim 0.003$) have been reported as well (e.g. Beckert & Duschl 2002; Yuan & Narayan 2014).

We can approximate the characteristic disk magnetic field strength by assuming that the equipartition magnetic pressure is half the gas pressure, viz., $B^2/8\pi = 0.5 \rho_i c_s^2$ where $c_s \simeq c(r_s/r)^{1/2}/\sqrt{3}$ is the sound speed. Though current simulations indicate some deviation from equipartition ($\beta_{ADAF} > 0.5$, cf. Yuan & Narayan 2014), this will provide a useful upper limit. With $4\pi r^2 \rho_i v_r = \dot{M}$ and radial inflow speed $v_r \simeq 0.5 \alpha_v v_f = (1/\sqrt{8}) \alpha_v (r_s/r)^{1/2} c$, where α_v is the viscosity coefficient, the disk magnetic field becomes $B_d \simeq 2.1 \times 10^4 \alpha_v^{-1/2} M_9^{-1/2} \dot{m}^{1/2} (r_s/r)^{5/4}$ G, which agrees well with previously reported ADAF results (e.g., Mahadevan 1997; Narayan et al. 1998; Yi 1999). Evaluating at characteristic radius $r = 1.5 r_g$ (Meier 2001) and using $\alpha_v = 0.1$ as reference value (e.g., King et al. 2007; Yuan & Narayan 2014), the inner disk field could thus reach strengths of

$$B_d \approx 10^5 \dot{m}^{1/2} M_9^{-1/2} \text{ G}. \quad (1)$$

Given that for ADAFs the disk scale height is about $H \sim r$, the strength of the poloidal magnetic field threading the black hole $B \simeq B_d \times (H/r)^n$, $n \sim 1$ (Livio et al. 1999; Meier 2001), is expected to be comparable in magnitude. In fact, taking the field-enhancing shear in the Kerr metric into account, the field threading the black hole may be a factor of about 2.3 larger (Meier 2001), i.e. $B_{d,h} \simeq 2.3 B_d$, which would bring it close to the value inferred from GRMHD jet simulations in the context of magnetically arrested disks (e.g., Tchekhovskoy et al. 2011; Tchekhovskoy & McKinney 2012; Yuan & Narayan 2014).

The emission spectrum of an ADAF is produced by synchrotron, inverse Compton and bremsstrahlung radiation of relativistic thermal electrons, and typically extends from radio frequencies up to hard X-rays (Narayan

& Yi 1995). Like any disk emission, this radiation constitutes a potential target for any magnetospheric VHE γ -rays. For sufficiently small accretion rate \dot{m} the peak energy ϵ_s and the luminosity L_s of the soft photon field become (Mahadevan 1997, viz. the synchrotron peak)

$$\epsilon_s \approx 0.2 \dot{m}^{3/4} M_9^{-1/2} T_{e,9}^2 \text{ eV}, \quad (2)$$

$$L_s \approx 5 \times 10^{43} \dot{m}^{9/4} M_9^{1/2} T_{e,9}^7 \text{ erg s}^{-1}, \quad (3)$$

where $T_{e,9} = T_e/10^9 \approx 5$ is the characteristic electron temperature which depends weakly on the accretion rate \dot{m} (Mahadevan 1997) and the radial distance r at the inner edge of the ADAF (Narayan & Yi 1995; Manmoto et al. 1997). For simplicity, we thus fix the temperature to $T_{e,9} = 5$ in all our following calculations. Correspondingly, the soft photon number density can be expressed as $n_s \simeq L_s/(2\pi r_s^2 c \epsilon_s) \approx 4 \times 10^{19} \dot{m}^{3/2} M_9^{-1} \text{ cm}^{-3}$.

Accreting black hole systems are capable of ejecting powerful jets. On average the maximum power of these jets, L_{jet} , should be comparable to the available accretion power $\dot{M}c^2$ (e.g., Ghisellini et al. 2014). This should also hold for ergospheric-driven (BZ) jets as the magnetic flux carried onto the black hole is proportional to \dot{M} (cf. eq. [1]). GRMHD simulations in fact show that the jet power does not exceed $\dot{M}c^2$ by more than a factor of ~ 3 (e.g., Tchekhovskoy et al. 2011). Hence, on phenomenological grounds one could write $L_{jet} = \xi \dot{M}c^2 = \xi L_{disk}/\eta_c = (\xi/\eta_c) \dot{m} L_{Edd}$ with $\xi \lesssim 3$. This could be related to the electromagnetic extraction of rotational energy of the supermassive black hole (Thorne et al. 1986). In the case of a rotating, force-free black hole magnetosphere (i.e., efficient energy extraction) the maximum Blandford-Znajek (BZ) jet power is given by

$$L_{BZ} = \Omega^F (\Omega^H - \Omega^F) B_\perp^2 \frac{r_H^4}{c} = (\Omega^F)^2 B_\perp^2 \frac{r_H^4}{c} \quad (4)$$

$$= \frac{1}{16} a_s^2 c r_H^2 B_\perp^2 \approx 2 \times 10^{48} \dot{m} M_9 \left(\frac{B_\perp}{B_{d,h}} \right)^2 \text{ erg s}^{-1},$$

where $\Omega^H = a_s c/2r_H$ is the black hole angular velocity, $\Omega^F = \Omega^H/2$ is the angular velocity of the field lines in the case of efficient extraction, and $B_\perp \simeq B_{d,h} \simeq 2.3B_d$ is the strength of the normal magnetic field component threading the event horizon $r_H = r_g (1 + \sqrt{1 - a_s^2}) \sim r_g$ (for $a_s \sim 1$). This concurs with the considerations above, $L_{BZ} = \xi \dot{M}c^2 \lesssim 4 \times 10^{48} \dot{m} M_9 \text{ erg/s}$, and suggesting that the BZ jet power provides a useful measure for \dot{M} and vice versa.

In general, magnetospheric VHE emission is perceived as a sub-product of an universal operation. If complete screening into the magnetosphere is not achieved ($\mathbf{E} \cdot \mathbf{B} \neq 0$), then particles, accelerated within the

gaps, are likely to emit multiple VHE radiation (e.g., Levinson 2000; Rieger 2011). Beyond an energy threshold, the VHE photons are absorbed by the ambient soft photon field producing secondary pairs. These will again be accelerated, their radiation being accompanied by further absorption/pair creation. In such a way, a photon-electron cascade is triggered, that guarantees a charge multiplicity such that force-freeness and MHD jet launching is ensured. Below the energy threshold, VHE photons can escape the black hole environment. Variable VHE emission observed from under-luminous AGN could thus signal the onset of relativistic jet formation (Levinson & Rieger 2011).

2.2. Gap electric field and potential

A quasi-steady magnetospheric gap can be formed in an under-dense environment ($n < n_{CJ}$). We consider in the following the gaps to be quasi-spherical, to be located at radial distance R_{gap} close to r_g , and to possess a size or extension denoted by h . The voltage drop or gap potential then scales with the gap size depending on how the fields and boundaries are treated and different description are thus encountered. As gaps are often expected to be thin ($h \ll r_g$), this could lead to substantial differences.

2.2.1. Heuristic constraint

A heuristic constraint might be obtained from the global electric field of a force-free magnetosphere, i.e. $\mathbf{E} = -\mathbf{V}/c \times \mathbf{B}$ in the high conductivity limit ($\sigma \rightarrow \infty$). Although the electric vector changes in the gap and only some part becomes parallel to the magnetic field lines, one may assume that its strength remains comparable in magnitude. Hence in order of magnitude, one could write for the electric field of the gap $E_{gap} \approx (V/c) B_{gap} \approx (\Omega^F R_{gap}/c) B_{gap}$ approximating $\sin \theta_b$ by unity. We note that this expression in principle assumes that charge sheets or charge injection occurs just outside the gap boundaries (cf. eq. [7] below). As this seems rather unexpected, the inferred E_{gap} should be considered as providing a clear upper limit for possible realisations.

Noting $E_{gap} \sim \Delta \mathcal{V}_{gap}/h$, where $\Delta \mathcal{V}_{gap}$ denotes the voltage drop, and using $\Omega^F \approx \Omega^H/2$ and $\Omega^H = c/2r_g$, one would obtain

$$\Delta \mathcal{V}_{gap} \approx \frac{1}{4} B_{gap} R_{gap} \left(\frac{h}{r_g} \right), \quad (5)$$

i.e. a voltage drop $\propto h$ scaling linearly with h (cf. in this context also Aharonian et al. 2017). Equation (5) then represents a fiducial upper limit for the voltage drop of the magnetospheric gap that can be tapped for the acceleration of particles. For $B_{gap} \simeq B_{d,h} \simeq 2.3B_d$

(eq. [1]) and $R_{gap} \sim r_g$ this would give

$$\Delta\mathcal{V}_{gap} \approx 2.5 \times 10^{21} \dot{m}^{1/2} M_9^{1/2} \left(\frac{h}{r_g} \right) \text{ Volts,} \quad (6)$$

noting that 1 Statvolt=300 Volts.

2.2.2. Physical estimation

Different scaling laws of the voltage drop with gap size h are in fact present in the literature. The apparent discrepancy can be related to different assumptions about the expected gap boundary conditions (see e.g., Beskin 2009). In its simplest (one-dimensional, non-relativistic) form the gap electric field along s in the presence of a non-zero charge density ρ_e may be determined from Gauss' law

$$\frac{dE_{||}}{ds} = 4\pi(\rho_e - \rho_{GJ}), \quad (7)$$

and the electrostatic potential from

$$\frac{d\Phi_e}{ds} = -E_{||}, \quad (8)$$

so that the voltage drop becomes $\Delta\mathcal{V}_{gap} = \Phi_e(s=h) - \Phi_e(s=0)$.

To specify the electric field an appropriate boundary condition needs to be chosen. We may distinguish two cases, i.e. a highly (case *i*) and a weakly (case *ii*) underdense one:

(i) Accordingly, case *i* can be characterized by $\rho_e \ll \rho_{GJ}$ and $E_{||}(s=0) \neq 0$, with the developing pair cascade ensuring that the field gets screened at scale height h , i.e. $E_{||}(s=h) = 0$. Thus, $dE_{||}/ds \approx -4\pi\rho_{GJ}$ and $E_{||} \approx -4\pi\rho_{GJ}s + const.$ (neglecting possible variations $\rho_{GJ}(s)$), so that using $E_{||}(s=h) = 0$ one can write

$$E_{||}(s) = 4\pi\rho_{GJ}(h-s) = 4\pi\rho_{GJ}h \frac{(h-s)}{h} = E_0 \frac{h-s}{h}, \quad (9)$$

with maximum $E_{||}(s=0) = E_0 = 4\pi\rho_{GJ}h$. The voltage or potential drop then becomes

$$\begin{aligned} \Delta\mathcal{V}_{gap} &= \int_0^h E_{||}(s) ds = -4\pi\rho_{GJ} \frac{h^2}{2} = -2\pi\rho_{GJ} h^2 \\ &= -2\pi\rho_{GJ} r_H^2 \left(\frac{h}{r_H} \right)^2 = \Phi_0 \left(\frac{h}{r_H} \right)^2, \quad (10) \end{aligned}$$

where $\Phi_0 \equiv -2\pi\rho_{GJ}r_H^2 \simeq \Omega^F r_H^2 B_{\perp}/c = \Omega^H r_H^2 B_{\perp}/(2c)$, with $\rho_{GJ} \simeq -\Omega^F B_{\perp}/(2\pi c)$, resulting in a scaling $\Delta\mathcal{V}_{gap} \propto h^2$ that is different to the one in eq. (5). Such a scaling, $\propto h^2$, figures most promising in the gap context (e.g., Blandford & Znajek 1977; Levinson 2000; Levinson & Rieger 2011). We note that in this case some continuous charge injection across the inner boundary

would be usually needed to keep the gap quasi-steady lest it to become intermittent. One could speculate that such a situation might arise close to the stagnation surface with the disk or corona facilitating plasma injection. Yet, given our limited understanding of the global magnetospheric structure for accreting black hole systems some caution needs to be exercised (see e.g., Contopoulos 2017). It seems thus useful to address this problem also from another side, i.e., to employ observational constraints to evaluate the possible relevance of different gap realisations, and this approach is pursued below (Sec. 3).

(ii) A different dependence is, however, obtained for case *ii*. Here, $\rho_e \sim \rho_{GJ}$ and hence $E_{||}(s=0) \approx 0$ with the cascade again ensuring that $E_{||}(s=h) = 0$. Note that even if initially $\rho_e = \rho_{GJ}$ somewhere, deviations are expected as $\rho_{GJ} \propto \cos\theta_b$ varies along field lines. For non-trivial $E_{||}$ the chosen boundary condition can only be satisfied if $dE_{||}/ds$ changes sign across the gap such that the electric field takes on an extremal value at $s=h/2$ (assuming symmetry), i.e., $dE_{||}/ds = 0$ at $s=h/2$, which by Gauss' law implies $\rho(h/2) = \rho_{GJ}(h/2)$. We can thus Taylor-expand the charge-density term $(\rho_e - \rho_{GJ}) \equiv \rho_{eff}$ around $s=h/2$ to give $\rho_{eff}(s) = \rho_{eff}(h/2) + \frac{d\rho_{eff}}{ds}|_{(h/2)}(s-h/2) = \frac{d\rho_{eff}}{ds}|_{(h/2)}(s-h/2) \equiv \rho'_{eff}(h/2)(s-h/2)$ noting that $\rho_{eff}(h/2) = 0$. Hence we have $dE_{||}/ds = 4\pi\rho'_{eff}(s-h/2)$ implying

$$E_{||}(s) = 4\pi\rho'_{eff} \left(\frac{1}{2}s^2 - \frac{hs}{2} \right) = -2\pi\rho'_{eff} r_H^2 \frac{s(h-s)}{r_H^2}. \quad (11)$$

In the case of the null surface we approximately have (e.g., Hirotani & Pu 2016)

$$\rho'_{eff}(h/2) \simeq -\frac{\rho_{GJ}}{r_H} \simeq \frac{\Omega^F B_{\perp}}{(2\pi cr_H)} \quad (12)$$

and hence

$$\begin{aligned} \Delta\mathcal{V}_{gap} &= \int_0^h E_{||}(s) ds = 4\pi\rho'_{eff} \left[\frac{1}{6}s^3 - \frac{1}{4}hs^2 \right]_0^h \\ &= -4\pi\rho'_{eff} \frac{h^3}{12} = -\frac{1}{3}\pi\rho'_{eff} r_H^3 \left(\frac{h}{r_H} \right)^3, \quad (13) \end{aligned}$$

implying a scaling $\propto h^3$ that is different from those previously discussed. It seems tempting to associate such a case in the astrophysical context with the region close to the null surface where the Goldreich-Julian charge density is expected to change sign. An analogous expression has been recently employed for studying the luminosity output of gaps in the AGN context (Hirotani & Pu 2016). The strength of case (ii) lies in the fact that it seemingly provides for a transparent self-consistent realisation of a quasi-steady gap (but cf. also Levinson & Segev 2017, for caveats).

To account for these differences and facilitate comparison, we employ a parametric expression in the following, i.e.

$$\begin{aligned} \Delta\mathcal{V}_{gap} &= \frac{1}{c} \eta \Omega^F r_H^2 B_\perp \left(\frac{h}{r_H} \right)^\nu \\ &\approx 2.5 \times 10^{21} \eta \dot{m}^{1/2} M_9^{1/2} \left(\frac{h}{r_g} \right)^\nu \text{ Volts, } (14) \end{aligned}$$

where the respective sets of numerical parameters η and ν are listed in Table (1), and where $B_{gap} \simeq B_{d,h}$ has been assumed for the second expression on the right hand side. Given the employed approximation (cf. case ii), this expression formally applies to thin gaps, though we only demand $h \leq r_g$ in the following.

2.3. Particle acceleration and VHE radiation

A charged particle, injected into the magnetospheric gap, will be strongly accelerated. Consider an electron of energy $E_e = \gamma_e m_e c^2$ experiencing the potential drop of equation (14). Its rate of energy gain per unit time is $d(\gamma_e m_e c^2)/dt = (c/r_g) e \Delta\mathcal{V}_{gap} (h/r_g)^{-1}$, where γ_e is the Lorentz factor of the electron, m_e is its rest mass and c is the speed of light. This implies a characteristic acceleration time scale $\tau_{acc} = E_e/(dE_e/dt)$ of

$$\tau_{acc}(\gamma_e) = 10^{-12} \frac{\dot{m}^{-1/2}}{\eta} M_9^{1/2} \gamma_e \left(\frac{h}{r_g} \right)^{1-\nu} \text{ s. } (15)$$

Electrons moving along field lines will, however, also experience losses due to field line curvature ("curvature radiation") and inverse Compton scattering (e.g., Rieger 2011, for a review). Assuming that the curvature radius is roughly equal to the gravitational one (i.e., $R_{cur} \approx r_g$), the cooling time scale due to curvature radiation becomes

$$\tau_{cur}(\gamma_e) \approx 4 \times 10^{30} M_9^2 \gamma_e^{-3} \text{ s. } (16)$$

The whole magnetosphere as well as the gap are embedded in the ambient soft photon field of the disk (see subsection 2.1). Electrons undergoing acceleration along the field will thus also Compton up-scatter these soft photons to multiple VHE energies where the occurrence of $\gamma\gamma$ -absorption can lead to the formation of a pair cascade (e.g., Levinson & Rieger 2011). To explore the characteristic inverse Compton (IC) cooling time scale we approximate the soft photon field as isotropic and quasi-monoenergetic with ϵ_s and L_s given by eqs. (2) and (3). The IC electron cooling time scale then follows (Aharonian & Atoyan 1981)

$$\begin{aligned} \tau_{ic}(\gamma_e) &= \frac{b^2}{3\sigma_T c n_s} \left[\left(6 + \frac{b}{2} + \frac{6}{b} \right) \ln(1+b) - \ln^2(1+b) \right. \\ &\quad \left. - 2 \text{Li} \left(\frac{1}{1+b} \right) - \frac{\frac{11}{12}b^3 + 8b^2 + 13b + 6}{(1+b)^2} \right]^{-1} \end{aligned} \quad (17)$$

where $\text{Li}(x) \equiv -\int_x^1 \ln y/(1-y) dy$ and $b \equiv b(\gamma_e) = 4\gamma_e \epsilon_s / (m_e c^2) \approx 3 \times 10^{-5} \dot{m}^{3/4} \gamma_e M_9^{-1/2}$ is a non-dimensional quantity.

An electron will quickly reach its terminal Lorentz factor at which energy gain is balanced by radiative losses. Using appropriate values of \dot{m} , M_9 , h , ν and equating the acceleration time with the cooling ones (i.e., $\tau_{acc} = \tau_{cur}$ or/and $\tau_{acc} = \tau_{ic}$), the maximum electron Lorentz factor γ_{max} can be explored. It is worth emphasising that both radiation processes will take place, though the shortest one will impose the relevant constraint. Hence we may write $\gamma_{max} = \min(\gamma_{cur}, \gamma_{ic})$, where the maximum particle Lorentz factor due to curvature is given by

$$\gamma_{cur} \approx 4.5 \times 10^{10} \eta^{1/4} \dot{m}^{1/8} M_9^{3/8} \left(\frac{h}{r_g} \right)^{\frac{\nu-1}{4}}. \quad (18)$$

In figure (1) the relevant time scales as a function of electron Lorentz factor are shown for a characteristic set of AGN parameters using the estimates in equations (15), (16) and (17). For the considered choice, IC losses are weakened by Klein-Nishina effects and maximum particle energies for all considered voltage drops are essentially constrained by curvature losses. Note however, that for smaller gap sizes $h/r_g < 0.5$, IC losses will start to become of relevance and reduce achievable electron energies, foremost for $\nu = 3$ (i.e. $\beta = 4$). Figure (1) suggests that maximum Lorentz factors of $\gamma_{max} \sim 10^{10}$ could in principle be reached. This in turn implies that IC photons could reach multi-TeV energies, $\epsilon_{ic} = \gamma_e m_e c^2 \leq 10^4$ TeV, while curvature emission could extend into the TeV regime, $\epsilon_{cur} = 3c\hbar \gamma_{max}^3 / (2R_{cur}) \sim 0.2 (\gamma_{max}/10^{10})^3 / M_9$ TeV. Magnetospheric gaps in AGN are thus putative VHE emitting sites. If proton injection into the gap would occur (e.g., via diffusion), with Lorentz factors limited by curvature losses, it is in principle conceivable that photo-meson ($p\gamma$) production in the soft photon field of the disk might contribute to this.

2.4. Gap luminosity

The radiative output of the gap depends on the number density of particles, n_\pm undergoing acceleration and radiation in the gap. Gap closure will occur once the effective charge density approaches the critical one, $|\rho_c| = e n_c$. This allows for an estimate of the maximum achievable VHE gap power L_{gap} given a voltage or potential drop $\Delta\mathcal{V}_{gap}$,

$$L_{gap} \simeq n_c V_{gap} \frac{dE_e}{dt} \simeq -\frac{|\rho_c|}{e} (2\pi r_H^2 h) \frac{e \Delta\mathcal{V}_{gap} c}{h}, \quad (19)$$

approximating the relevant gap volume, V_{gap} , by a half-sphere of gap height h . The appropriate ρ_c or n_c to be

Table 1. Gap voltage and luminosity parameters

Exponent ν	Coefficient η	Coefficient β	Reference
1	1	1	[1]
2	1	2	[2-4]
3	1/6	4	[5]

NOTE—Parameters η and ν for the voltage drop scaling $\Delta\mathcal{V}_{gap} \propto \eta (h/r_H)^\nu$ as defined in equation (14) and the corresponding maximum luminosity output $L_{gap} \propto L_{BZ} (h/r_H)^\beta$ following equation (20). The first column specifies the power dependence on h , the second and third the corresponding values for η and β respectively, and the fourth gives exemplary references, with [1] = current work (reference limit), [2] Blandford & Znajek (1977), [3] Levinson (2000), [4] Levinson & Rieger (2011), [5] Hirotani & Pu (2016).

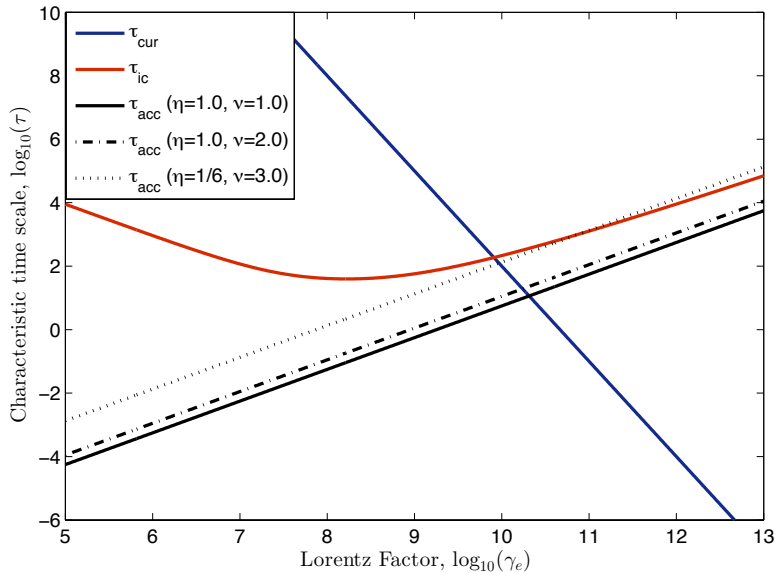


Figure 1. Characteristic time scales as a function of Lorentz factor γ_e for $M_9 = 5$, $\dot{m} = 10^{-4}$, $h/r_g = 0.5$. The solid blue line and red curve represent the time scales for curvature and inverse Compton losses, respectively. The (rising) black lines represent the acceleration time scales for the different gap potentials. The intersection points provide a measure of the achievable maximum energies.

employed are dependent on the assumed gap set-up. For the heuristic and under-dense cases ($\nu = 1$ and $\nu = 2$ as delineated above, cf. eq. [14]), the critical value is typically comparable to the Goldreich-Julian density, i.e. $\rho_c = \rho_{GJ} \simeq -\Omega^F B_\perp / (2\pi c) = -\Omega^H B_\perp / (4\pi c)$. In the weakly under-dense case ($\nu = 3$), however, the appropriate value based on eq. (12) instead is $\rho_c \simeq \rho'_{eff} h \simeq \rho_{GJ} h/r_H$ (e.g., Hirotani & Pu 2016). This results in scaling for the gap power $L_{gap} \propto h^4$ with power index increased by one compared to the respective potential drop (eq. [13]), while the index remains the same for the former cases.

Since $L_{gap} \propto (\Omega^F)^2 B_\perp^2$ we can also express the respective gap luminosity in terms of the Blandford-Znajek jet power, eq. (5). This gives

$$L_{gap} = \eta L_{BZ} \left(\frac{h}{r_H} \right)^\beta \lesssim L_{BZ}, \quad (20)$$

where the respective sets of parameters are listed in Table (1). For gap sizes $h \ll r_g$ then, the expected VHE output is much smaller than the jet power.

2.5. Accretion environment

Independent of the preferred gap formation scenario, to avoid external $\gamma\gamma$ -absorption of the gap-produced

VHE gamma-rays and facilitate their escape from the vicinity of a supermassive black hole, magnetospheric models generally require an under-luminous or radiatively inefficient (RIAF) inner disk environment. For suppose that the disk would be of an (un-truncated) standard (geometrically thin, optically thick) type, for which the effective surface temperature obeys (e.g., Frank, King & Raine 2002)

$$T_{\text{eff}}(r) = \left[\frac{3GM\dot{M}}{8\pi\sigma r^3} \left(1 - \sqrt{\frac{r_{\text{in}}}{r}} \right) \right]^{1/4} = 3.5 \times 10^5 \\ \times \dot{m}^{1/4} M_9^{-1/4} \left(\frac{r_s}{r} \right)^{3/4} \left(1 - \sqrt{\frac{r_{\text{in}}}{r}} \right)^{1/4} \quad \text{K} \quad (21)$$

with σ the Stefan Boltzmann constant. This profile peaks at a temperature $T_p \simeq 0.5 (3GM\dot{M}/8\pi\sigma r^3)^{1/4}$ close to the inner disk radius $r \sim r_{\text{in}} \sim r_s$ and exhibits the canonical $r^{-3/4}$ dependence. For characteristic AGN parameters, the peak of the thermal disk emission, carrying a power of order $L_{\text{disk}} = \dot{m}L_{\text{Edd}}$, would then be occurring at eV energies, i.e., $\epsilon_p \simeq 2.8kT_p \simeq 40 \dot{m}^{1/4} M_9^{-1/4}$ eV. This thermal disk radiation field would then provide an ideal target for the absorption of VHE photons producing pairs via $\gamma\gamma_{\text{VHE}} \rightarrow e^+e^-$. VHE photons of energy ϵ_γ , in fact, interact most efficiently with ambient soft photons of energy (e.g., Rieger 2011)

$$\epsilon_d \simeq 1 \left(\frac{1 \text{ TeV}}{\epsilon_\gamma} \right) \text{ eV}. \quad (22)$$

The corresponding optical depth is of order $\tau_{\gamma\gamma} \sim \sigma_{\gamma\gamma} n_d r$. With $\sigma_{\gamma\gamma} \simeq 0.2\sigma_T$ and $n_d \sim L_d/4\pi r^2 c\epsilon_d$, approximating $L_d \simeq L_{\text{disk}} \times (\epsilon_d/\epsilon_p)^3$ (Rayleigh-Jeans limit) and $r \sim r_s$, this would be of the order of

$$\tau_{\gamma\gamma} \sim 10^3 \dot{m}^{1/4} M_9^{3/4} \gg 1, \quad (23)$$

for VHE photons, i.e. greatly exceeding unity for conventional AGN parameters (cf. also Zhang & Cheng 1997). Hence, even if the black hole magnetosphere would produce VHE radiation via some gap mechanism, most of it is expected to become absorbed unless the disk would be of a radiatively inefficient (RIAF/ADAF) type where $L_d = L_{\text{ADAF}} \ll L_{\text{disk}}$ and the dominant part is emitted at energies much below 1 eV, cf. eq. (2). Very low accretion rates, or conservatively, the presence of a RIAF or ADAF thus becomes a necessary (yet not in itself sufficient) condition for the detectability of magnetospheric VHE emission in AGN. An ADAF-type (optically-thin) accretion flow with $H \sim r$ could also ensure the necessary poloidal magnetic field strength for efficient BZ power extraction (e.g., Livio et al. 1999; Meier 2001).

3. APPLICATION

Gap-driven magnetospheric emission processes have been suggested as a potential generator of the highly variable VHE radiation seen from misaligned, non-blazar AGNs (e.g., Neronov & Aharonian 2007; Levinson & Rieger 2011; Aleksić et al. 2014a; Vincent 2015; Ptitsyna & Neronov 2016; Hirotani & Pu 2016). In this section, we seek to assess the potential of such scenarios on quite general grounds, putting the relevant variability, transparency and power constraints in context.

First, VHE flux variability on short timescales Δt will limit the size of the putative gap to $h \lesssim c\Delta t$. We generally expect h to not exceed r_g if efficient pair cascade formation occurs. VHE flux variability thus imposes a limit on the extractable gap power as $L_{\text{gap}} \propto L_{\text{BZ}}(h/r_g)^\beta$, see eq. (20). On the other hand, to ensure transparency, i.e. for magnetospheric VHE emission to become observable, a radiatively inefficient disk (ADAF) environment is required (see subsection 2.5). This requires the accretion rate to satisfy $\dot{m} \lesssim \dot{m}_c$ and in turn leads to a constraint on the average jet power $L_{\text{jet}} \sim L_{\text{BZ}} \propto \dot{m}$, cf. eq. (5). Though a variety of values for \dot{m}_c have been reported, $\dot{m}_c \sim 0.01$ appears to be a representative upper limit (e.g., Yuan & Narayan 2014). Following this line of reasoning and assuming a rapidly spinning black hole, the constraints on the gap size and accretion rate thus translate into a characteristic upper-limit on the extractable VHE gap power of

$$L_{\text{gap}}^{\text{VHE}} \lesssim 2 \times 10^{46} \eta \left(\frac{\dot{m}_c}{0.01} \right) \left(\frac{M_{\text{BH}}}{10^9 M_\odot} \right) \\ \times \min \left\{ \left(\frac{c\Delta t}{r_g} \right)^\beta, 1 \right\} \text{ erg s}^{-1}. \quad (24)$$

We note that this expression provides a quite general constraint and does not as yet presuppose a specific mechanism for pair injection. Under quasi-steady circumstances and provided that the flow is hot enough ($kT_e/m_e c^2 \sim 1$), annihilation of MeV bremsstrahlung photons could well lead to a charge density in excess of ρ_{GJ} before \dot{m} approaches the critical value \dot{m}_c (Levinson & Rieger 2011). This would then introduce a further constraint on \dot{m} as to the possible existence of a gap. For typical two-temperature models $T_e \gtrsim 100$ keV is expected (Yuan & Narayan 2014). However, uncertainties in the electron temperature T_e caused by uncertainties in the electron heating parameters (in particular concerning the viscous dissipation that heats the electrons) along with flow intermittencies can introduce significant uncertainties in the pair production rate. At low accretion rates, early results, for example, suggested that $T_e \propto \dot{m}^{-q}$ with $0 \lesssim q \lesssim 0.2$ (e.g., Mahadevan 1997; Esin

et al. 1997), leading to some further ambiguity concerning pair processes. Note that the scaling in equation (24) formally applies to small h/r_g and that we have used $h \sim r_g$ for a representative upper limit. In principle a full general relativity model (e.g., Levinson & Segev 2017) would be needed to self-consistently evaluate possible gap widths.

In Fig. (2), the product $P = 10^{-48} L_{gap} M_9^{-1} (h/r_g)^{-\beta}$ with $h \leq r_g$, which provides a normalized measure of the maximum gap power for a given black hole mass and gap size, is shown as function of accretion rate (or correspondingly, magnetic field strength threading the horizon, $B \propto \dot{m}^{1/2}$, cf. eq. (1)). The case of a highly ($\eta = 1$) and weakly ($\eta = 1/6$) under-dense gap are given by the dotted and dash-dotted line, respectively. Observed VHE gamma-ray powers that are above these lines are unlikely to originate in (quasi steady) magnetospheric gaps. Both lines preserve their meaning for accretion rate lower than the critical one. These considerations are applied in the following to the most prominent candidate sources.

3.1. M87

The Virgo Cluster radio galaxy M87 (NGC 4486), located at a distance of $d \simeq 16.7$ Mpc (Mei et al. 2007) and believed to harbour a black hole of mass $M_{BH} = (2 - 6) \times 10^9 M_\odot$, has been the first extragalactic source detected at VHE energies (Aharonian et al. 2003). Given its proximity, M87 has been a prime target to probe scenarios for the formation of relativistic jets with high-resolution radio observations exploring scales down to some tens of r_g and much effort has been recently dedicated into this direction (e.g., Acciari et al. 2009; Doeleman et al. 2012; Hada et al. 2014, 2016; Kino et al. 2015; Akiyama et al. 2015, 2017). At VHE energies, M87 has revealed at least three active γ -ray episodes during which day-scale flux variability (i.e., $h = c\Delta\tau_{obs} \sim r_g$) has been observed (Aharonian et al. 2006; Albert et al. 2008; Acciari et al. 2009; Abramowski et al. 2012; Aliu et al. 2012). The VHE spectrum is compatible with a relatively hard power-law (photon index ~ 2.2) extending from 300 GeV to beyond 10 TeV, while the corresponding TeV output is relatively moderate, with an isotropic equivalent luminosity of $L_{VHE} \simeq (3 - 10) \times 10^{40}$ ergs $^{-1}$. The inner, pc-scale jet in M87 is considered to be misaligned by $i \sim (15 - 25)^\circ$, resulting in modest Doppler boosting of its jet emission and creating challenges for conventional jet models to account for the observed VHE characteristics (see e.g., Rieger & Aharonian 2012, for review and references). Gap-type emission models offer a promising alternative and different realisations have

been proposed in the literature (e.g., Neronov & Aharonian 2007; Levinson & Rieger 2011; Vincent 2015; Broderick & Tchekhovskoy 2015; Ptitsyna & Neronov 2016). M87 is overall highly under-luminous with characteristic estimates for its total nuclear (disk and jet) bolometric luminosity not exceeding $L_{bol} \simeq 10^{42}$ ergs $^{-1}$ by much (e.g., Owen et al. 2000; Whysong & Antonucci 2004; Prieto et al. 2016), suggesting that accretion onto its black hole indeed occurs in a non-standard, advective-dominated (ADAF) mode characterized by an intrinsically low radiative efficiency (e.g., Di Matteo et al. 2003; Nemmen et al. 2014), with inferred accretion rates possibly ranging up to $\dot{m} \sim 10^{-4} \ll \dot{m}_c$ (e.g., Levinson & Rieger 2011) and black hole spin parameter close to its maximum one (e.g., Feng & Wu 2017). For these values of the accretion rate, the soft photon field, cf. eqs. (2) and (3), is sufficiently sparse, so that the maximum Lorentz factor $\gamma_e \sim 10^{10}$ of the magnetospheric particles is essentially determined by the curvature mechanism. The observed VHE variability is in principle compatible with $h \sim r_g$, so that the different dependence of the gap power on β , eq. (20), does not necessarily (in the absence of other, intrinsic gap closure considerations) imply a strong difference in the extractable gap powers. Fig. (2) shows a representative point for M87 (taking $\beta = 1$). The observed VHE luminosity of M87 is some orders of magnitudes lower than the maximum possible gap power (given by the dotted line) and within the bound imposed by ADAF considerations (vertical line). The observed VHE flaring events thus appear consistent with a magnetospheric origin. VLBI observations of (delayed) radio core flux enhancements indeed provide support for the proposal that the variable VHE emission in M87 originates at the jet base very near to the black hole (e.g., Acciari et al. 2009; Beilicke et al. 2012; Hada et al. 2012, 2014).

3.2. IC 310

The Perseus Cluster galaxy IC310 (J0316+4119) has revealed remarkable VHE variability during a strong flare in November 2012, exhibiting VHE flux variations on timescales as short as $\Delta t \simeq 5$ min (Aleksić et al. 2014a). IC310 is located at a distance of $d \sim 80$ Mpc ($z=0.019$) and widely believed to harbour a black hole of mass $M_{BH} \simeq 3 \times 10^8 M_\odot$ (Aleksić et al. 2014a, but cf. also Berton et al. (2015) for a ten times smaller estimate). The flare spectrum in the energy range 70 GeV to 8.3 TeV appears compatible with a hard power law of photon index $\Gamma \simeq 2$ and does not show indications for internal absorption. The observed VHE fluxes can reach levels corresponding to an isotropic-equivalent luminosity of $L_{VHE} \simeq 2 \times 10^{44}$ ergs $^{-1}$. A variety of

considerations based on the orientation of the jet in IC310 (probably $i \sim 10 - 20^\circ$), on kinetic jet power and timing constraints has led [Aleksić et al. \(2014a\)](#) to disfavour alternative proposals for fast VHE variability, such as jet-star interaction (e.g., [Barkov et al. 2012](#)) or magnetic reconnection (e.g. [Giannios 2013](#)). Detailed investigation, however, suggests that this does not have to be the case (cf. [Aharonian et al. 2017](#), for details). Nevertheless, the fact that the VHE flux varies on timescales Δt much shorter than the light travel time across black hole horizon scales, $r_g(3 \times 10^8 M_\odot)/c = 25$ min, has been interpreted as evidence for the occurrence of gap-type particle acceleration on sub-horizon scales, i.e. of gap height $h \simeq 0.2r_g$ (e.g., [Aleksić et al. 2014a](#); [Hirotani & Pu 2016](#)). To sustain a steady, isotropic equivalent luminosity of $L_{bol} \sim 10^{44}$ ergs $^{-1}$, the average jet power should satisfy $L_j \gtrsim 10^{42} (\theta_j/0.3 \text{ rad})^2$ ergs $^{-1}$ (cf. also, [Sijbring & de Bruyn 1998](#); [Ahnen et al. 2017](#)), where θ_j denotes the jet opening angle, suggesting that typical accretion rates should exceed $\dot{m} \gtrsim 10^{-5} M_8^{-1}$ (where $M_8 = M_{BH}/10^8 M_\odot$). Taking such a jet power as a reference, the expected gap emission would strongly under-predict the required VHE luminosity, see eq. (20). As $L_{gap}^{VHE} \propto B^2$ the gap would need to be temporarily threaded by much higher magnetic fields, and accordingly require much higher accretion rates, cf. eq. (1). If $h \sim r_g$ accretion rates of the order of $\dot{m} \sim 10^{-3}$ might seemingly be sufficient. The variability constraint $h \sim 0.2r_g$, however, implies that $L_{gap}^{VHE} \lesssim 6 \times 10^{45} \eta (\dot{m}_c/0.01) (0.2)^\beta$ ergs $^{-1}$, see eq. (24). This results in $L_{gap}^{VHE} \lesssim 2 \times 10^{44}$ ergs $^{-1}$ for the $\beta = 2$ with $\eta = 1$, and $L_{gap}^{VHE} \lesssim 10^{42}$ ergs $^{-1}$ assuming $\beta = 4$ with $\eta = 1/6$, see table 1. In Fig. (2), two representative points (i.e., for $\beta = 1$ and $\beta = 4$) illustrating the range for IC310 are shown. While the case with $\beta = 2$ may appear marginally possible, we note that for accretion rates approaching \dot{m}_c the existence of a gap is not guaranteed. In fact, annihilation of ADAF bremsstrahlung photons is likely to lead to an injection of pairs in excess of the Goldreich-Julian density, $n_\pm/n_{GJ} \sim 3 \times 10^{12} \dot{m}^{7/2}$ ([Levinson & Rieger 2011](#), eq. (8)), suggesting that rates $\dot{m} \lesssim 3 \times 10^{-4}$ are needed to avoid gap closure. Even for the most optimistic case ($\beta = 1$), the maximum gap power, eq. (24), is then not expected to exceed $L_{gap}^{VHE} \sim 4 \times 10^{43}$ ergs $^{-1}$. We note that this concurs with a similar estimate in [Aharonian et al. \(2017\)](#). This would imply that the noted VHE flaring event cannot be of a gap-type magnetospheric origin independent of the assumed power index β . A putative way out could be to assume an inner electron temperature $kT_e/(m_e c^2) < 1$ such that bremsstrahlung emission would be suppressed at MeV

energies thereby possibly relaxing the pair-injection constraint on \dot{m} . Whether this is feasible in the case of IC310 would need detailed disk modelling. But beside of this, the apparently huge magnetic fields required to thread the gap ($B_{d,h} \sim 2 \times 10^5$ G in the case of $\beta = 4$) would suggest a temporary increase in accretion rate in excess of \dot{m}_c required for the existence of an ADAF. This, then, would make it again unlikely that magnetospheric VHE emission from IC310 should become observable, see Sec. 2.5. The situation might, however, be more complex as unsteady accretion and strong intermittency could be occurring. In the case of IC310 the ~ 5 min flare event detected during 3.7 hrs of MAGIC observations in the night November 12-13, 2012, however, seems part of a higher source state, probably (considering earlier 2009/10 results) of day-scale duration t_d ([Aleksić et al. 2014a](#); [Aleksić et al. 2014b](#); [Ahnen et al. 2017](#)). If one takes the timescale t_{th} for re-adjustment of thermal equilibrium as characteristic measure, $t_{th} \sim t_{dyn}/\alpha_v \sim 1/(\alpha_v \Omega_k) \sim \alpha_v^{-1} (r/r_g)^{3/2} r_g/c \sim 4 (r/r_g)^{3/2}$ hr $\lesssim t_d$, then this could be occurring sufficiently fast to ensure re-adjustment of the innermost disk parts. Another situation would be arising if the black hole mass in IC310 would indeed be smaller by an order of magnitude, i.e. $M_{BH} \sim 3 \times 10^7 M_\odot$, as suggested by [Berton et al. \(2015\)](#). The observed rapid VHE variability of $\Delta t \sim 5$ min would then only imply $h \sim r_g$, such that the different dependence on β , e.g. eq. (24), would not make a significant difference. The limit introduced by eq. (24) would then suggest that the observed VHE output might be formally achieved (assuming $\dot{m} \sim 0.01$). However, for such a rate and given the small black hole mass, eq. (2) would imply a synchrotron peak around $\epsilon_s \sim 1$ eV with associated power L_s such, that the VHE photons are unlikely to escape absorption. In summary, though one could speculate that on r_g -scales the accretion flow evolves in a highly turbulent way, thereby changing its radiative characteristics, a gap-driven magnetospheric origin for the recent VHE flaring event in IC310 appears to be disfavoured unless its black hole mass and accretion state would be highly different.

4. CONCLUSION

Gap-driven magnetospheric gamma-ray emission from rotating supermassive black holes is a potential candidate for the origin of the highly variable VHE emission seen in some AGN (e.g., [Rieger 2011](#), for review). The presence of strong, unscreened parallel electric field components on black hole horizon scales $\sim r_g$ could easily facilitate efficient particle acceleration, with the accompanying curvature and inverse Compton processes resulting in appreciable emission at gamma-ray energies.

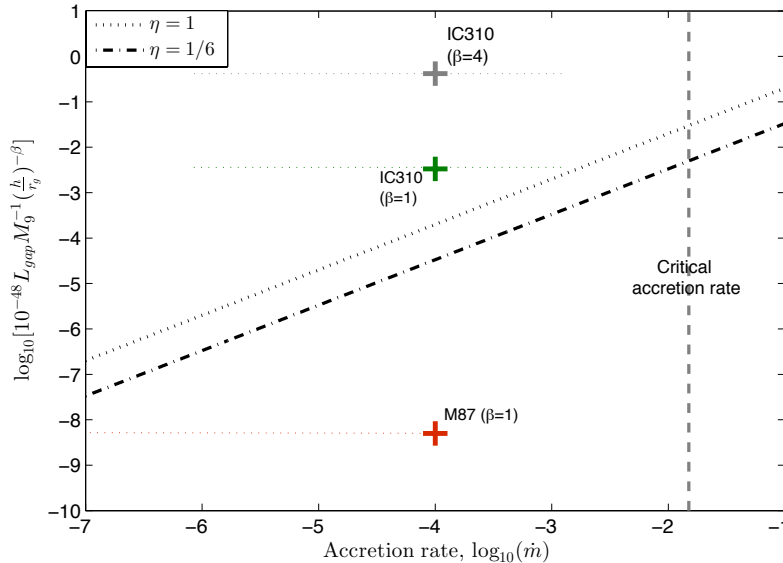


Figure 2. Characteristic maximum power of a magnetospheric gap as a function of accretion rate \dot{m} . The dotted and dash-dotted lines represent the maximum for $\eta = 1$ and $\eta = 1/6$, respectively. Observed gamma-ray powers below these limiting lines could in principle be produced by magnetospheric gaps.

The efficiency and extractable power, however, depend on details of the gap set-up and different realizations are in principle conceivable and encountered in the literature. The present work explores possible implications of this by means of a simple phenomenological description that though heuristic, recovers the relevant dependencies. Accordingly, the maximum extractable gap power is in general proportional to the classical Blandford-Znajek jet power, $L_{BZ} \propto \dot{m} M_{BH}$, and a function of the gap height h , $L_{gap} \sim L_{BZ} (h/r_g)^\beta$, where the power index β is dependent on the respective gap-setup (cf. Table 1). In order for this emission to become observable, VHE photons need to be able to escape the accretion environment of the black hole. Transparency to $\gamma\gamma$ -pair production in fact requires an under-luminous or radiatively inefficient environment (RIAF/ADAF), and this introduces a relevant constraint on possible accretion rates of $\dot{m} \lesssim 0.01$. While for a fixed background a larger black hole mass (size) could be conducive to dilution of the soft photon field (facilitating VHE transparency) and increase L_{BZ} , the detection of rapid gamma-ray variability with $c\Delta t \sim h < r_g$ reduces the maximum gap power $L_{gap}^{VHE} \propto M_{BH}^{1-\beta}$ (for $\beta > 1$) and diminish the VHE prospects for source detection. When put in the context of current observations, these considerations suggest that the variable (day-scale) VHE activity seen in the radio galaxy M87 ($M_{BH} \simeq [2 - 6] \times 10^9 M_\odot$) may be compatible with a magnetospheric origin, while such an origin seems less likely for the (minute-scale) VHE

activity in IC310 (assuming $M_{BH} \simeq 3 \times 10^8 M_\odot$).

Our analysis implies that variability information will be crucial to get deeper insights into the physics of the putative gaps, to probe different potential scalings and to generally assess the plausibility of a magnetospheric origin. On average, however, (quasi steady) magnetospheric VHE gamma-ray emission in AGN is expected to be of rather moderate luminosity when compared to the strongly Doppler-boosted jet emission from blazars. The jet usually needs to be sufficiently misaligned for the gap emission not to be masked by Doppler-boosted jet emission, making nearby misaligned AGN the most promising source targets. The possible impact of intermittencies in the gap formation process (e.g., Levinson & Segev 2017) on the VHE characteristics could be of particular interest in this regard. The increase in sensitivity with the upcoming CTA instrument will allow to probe variability timescales $< r_g/c$ for a number of these sources, and thereby allow a better census of magnetospheric gamma-ray emitter.

Acknowledgments

GK kindly acknowledges support by an IMPRS Fellowship. FMR kindly acknowledges financial support by a DFG Heisenberg Fellowship (RI 1187/4-1). We are grateful to A. Levinson for comments on early version of the manuscript. Discussions with F. Aharonian, K. Mannheim, C. Fendt, D. Khangulyan and D. Glawion are gratefully acknowledged.

REFERENCES

- Abramowski, A., Acero, F., Aharonian, F., et al. 2012, *ApJ*, 746, 151
- Acciari, V. A., Aliu, E., Arlen, T., et al. 2009, *Science*, 325, 444
- Acero, F., Ackermann, M., Ajello, M., et al. 2015, *ApJS*, 218, 23
- Ackermann, M., Ajello, M., Atwood, W.B., et al. 2015, *ApJ*, 810, 14
- Aharonian, F., Akhperjanian, A., Beilicke, M., et al. 2003, *A&A*, 403, L1
- Aharonian, F. A., Atoyan, A. M., 1981, *Ap&SS*, 79, 321
- Aharonian, F. A., Belyanin, A. A., Derishev, E. V., Kocharovskiy, V. V., Kocharovskiy, V. V., 2002, *PhRvD*, 66, 023005
- Aharonian, F., Akhperjanian, A. G., Bazer-Bachi, A. R., et al. 2006, *Science*, 314, 1424
- Aharonian, F. A., Barkov, M. V., Khangulyan, D., 2017, *ApJ*, 841, 61
- Ahnen, M.L., Ansoldi, S., Antonelli, L.A., et al. 2017, *A&A*, 603, A25
- Akiyama, K., Lu, R.-S., Fish, V.L., et al. 2015, *ApJ*, 807, 150
- Akiyama, K., Kuramochi, K., Ikeda, S., et al. 2017, *ApJ*, 838, 1
- Albert, J., Aliu, E., Anderhub, H., et al. 2008, *ApJ*, 685, L23
- Aleksić, J., Ansoldi, S., Antonelli, L. A., et al. 2014a, *Science*, 346, 1080
- Aleksić, J., Antonelli, L. A., Antoranz, P., et al. 2014b, *A&A*, 563, A91
- Aleksić, J., Antonelli, L. A., Antoranz, P., et al. 2010, *ApJL*, 723, L207
- Aliu, E., Arlen, T., Aune, T., et al. 2012, *ApJ*, 746, 141
- Barkov, M. V., Aharonian, F.A., Bosch-Ramon, V., 2010, *ApJ*, 724, 1517
- Barkov, M. V., Aharonian, F. A., Bogovalov, S. V., Kelner, S. R., Khangulyan, D., 2012, *ApJ*, 749, 119
- Beckert, T., Duschl, W. J., 2002, *A&A*, 387, 422
- Beilicke, M., VERITAS Collaboration, 2012, *American Institute of Physics Conference Series* (ed. F. A. Aharonian, W. Hofmann & F. M. Rieger), vol. 1505, pp. 586
- Berton, M., Foschini, L., Ciroi, S., et al. 2015, *A&A*, 578, A28
- Beskin, V. S., 2009, *MHD Flows in Compact Astrophysical Objects: Accretion, Winds and Jets* (Springer)
- Beskin, V. S., Istomin, Y. N., Pared, V. I., 1992, *Sov. Astr. Lett.*, 36, 642
- Beskin, V. S., Kuznetsova, I. V., 2000, *Nuovo Cimento B Serie*, 115, 795
- Blandford, R. D., Znajek, R. L., 1977, *MNRAS*, 179, 433
- Boldt, E., & Ghosh, P., 1999, *MNRAS*, 307, 491
- Boldt, E., Loewenstein, M., 2000, *MNRAS*, 316, L29
- Broderick, A. E., Tchekhovskoy, A., 2015, *ApJ*, 809, 97
- Contopoulos, I. 2017, *MNRAS in press* (arXiv:1711.00302)
- Di Matteo, T., Allen, S. W., Fabian, A. C., Wilson, A. S., Young, A. J., 2003, *ApJ*, 582, 133
- Doeleman, S. S., Fish, V. L., Schenck, D. E., et al. 2012, *Science*, 338, 355
- Esin, A. A., McClintock, J. E., Narayan, R., 1997, *ApJ*, 489, 865
- Feng, J., Wu, Q., 2017, *MNRAS*, 470, 612
- Frank, J., King, A., Raine, D., 2002, *Accretion Power in Astrophysics* (CUP)
- Giannios, D., Uzdensky, D.A., Begelman, M. C., 2010, *MNRAS*, 402, 1649
- Giannios, D., 2013, *MNRAS*, 431, 355
- Ghisellini, G., Tavecchio, F., Maraschi, L., Celotti, A., Sbarrato, T., 2014, *Nature*, 515, 376
- Globus, N., Levinson, A., 2014, *ApJ*, 796, 26
- Hada, K., Giroletti, M., Kino, M., et al. 2014, *ApJ*, 788, 165
- Hada, K., Kino, M., Nagai, H., et al. 2012, *ApJ*, 760, 52
- Hada, K., Kino, M., Doi, A., et al. 2016, *ApJ*, 817, 131
- Hirovani, K., Okamoto, I., 1998, *ApJ*, 497, 563
- Hirovani, K., Pu, H.-Y., 2016, *ApJ*, 818, 50
- Hirovani, K., Pu, H.-Y., Lin, L. C.-C., et al. 2016, *ApJ*, 833, 142
- Kalashov, O. E., Ptitsyna, K. V., Troitsky, S. V., 2012, *PhRvD*, 86, 063005
- King, A. R., Pringle, J. E., Livio, M., 2007, *MNRAS*, 376, 1740
- Kino, M., Takahara, F., Hada, K., et al. 2015, *ApJ*, 803, 30
- Lenain, J.-P., Boisson, C., Sol, H., Katarzyński, K., 2008, *A&A*, 478, 111
- Levinson, A., 2000, *ApJ*, 85, 912
- Levinson, A., & Boldt, E., 2002, *Astroparticle Physics*, 16, 265
- Levinson, A., Rieger, F., 2011, *ApJ*, 730, 123
- Levinson, A., & Segev, N., 2017, (arXiv:1709.09397)
- Livio, M., Ogilvie, G. I., Pringle, J. E., 1999, *ApJ*, 512, 100
- Mahadevan, R., 1997, *ApJ*, 477, 585
- Manmoto, T., Mineshige, S., Kusunose, M., 1997, *ApJ*, 489, 791
- Mei, S., Blakeslee, J. P., Côté, P., et al. 2007, *ApJ*, 655, 144
- Meier, D. L., 2001, *ApJL*, 548, L9

- Moncada, R. J., Colon, R. A., Guerra, J. J., O'Dowd, M. J., Anchordoqui, L. A., 2017, *Journal of High Energy Astrophysics*, 13, 32
- Narayan, R., Mahadevan, R., Quataert, E., 1998, in: *The Theory of Black Hole Accretion Disks*, ed. M.A. Abramowicz et al. (Cambridge Univ. Press), 148
- Narayan, R., Yi, I., 1995, *ApJ*, 452, 710
- Nemmen, R. S., Storchi-Bergmann, T., Eracleous, M., 2014, *MNRAS*, 438, 2804
- Neronov, A., Aharonian, F. A., 2007, *ApJ*, 671, 85
- Neronov, A. Y., Semikoz, D. V., Tkachev, I. I., 2009, *New Journal of Physics*, 11, 065015
- Osmanov, Z., Mahajan, S., Machabeli, G., 2017, *ApJ*, 835, 164
- Owen, F. N., Eilek, J. A., Kassim, N. E., 2000, *ApJ*, 543, 611
- Pedaletti, G., Wagner, S. J., Rieger, F. M., 2011, *ApJ*, 738, 142
- Prieto, M. A., Fernández-Ontiveros, J. A., Markoff, S., Espada, D., González-Martín, O., 2016, *MNRAS*, 457, 3801
- Ptitsyna, K., Neronov, A., 2016, *A&A*, 593, A8
- Rieger, F., Aharonian, F. A., 2008, *A&A*, 479, L5
- Rieger, F. M., Aharonian, F., 2012, *Modern Physics Letters A*, 27, 1230030
- Rieger, F., 2011, *Int. J. Mod. Phys. D*, 20, 1547
- Rieger, F. M., 2017, *American Institute of Physics Conference Series* (ed. F. A. Aharonian, W. Hofmann & F. M. Rieger), vol. 1792, 020008
- Sijbring, D., de Bruyn, A. G., 1998, *A&A*, 331, 901
- Tavecchio, F., Ghisellini, G., 2008, *MNRAS*, 385, L98
- Thorne, K. S., Price, R. H., MacDonald, D. A., 1986, *Black Holes: The Membrane Paradigm*, (Yale Univ. Press)
- Tchekhovskoy, A., Narayan, R., McKinney, J., 2011, *MNRAS*, 418, L79
- Tchekhovskoy, A., McKinney, J. C., 2012, *MNRAS*, 423, L55
- Vincent, S., LeBohec, S., 2010, *MNRAS*, 409, 1183
- Vincent, S., 2015, *JCAP*, 05, 042
- Wald, R. M., 1974, *PhRvD*, 10, 1680
- Whysong, D., Antonucci, R., 2004, *ApJ*, 602, 116
- Yuan, F., Narayan, R., 2014, *ARA&A*, 52, 529
- Yi, I., 1999, in: *Astrophysical Discs*, eds. J.A. Sellwood and J. Goodman, *ASP Conf. Series*, 160, 279
- Zhang, L., Cheng, K. S., 1997, *ApJ*, 475, 534